IEEE Robotics and Automation Letters (RA-L) paper, presented at ICRA 2024, Yokohama, Japan. Cite as RA-L paper.

A Power-Aware Control Strategy for an Elbow Effort-Compensation Device

Emir Mobedi[1,2], Sebastian Hjorth[3], Wansoo Kim[4], Elena De Momi[2], Nikos G. Tsagarakis[1], and Arash Ajoudani[1]

***Abstract*—This work presents a reactive control strategy for loading and sudden unloading of an elbow effort-compensation device controlled in force. Through this control strategy, in addition to an individual's forearm weight, an external load can be detected and adaptively compensated via a feed-forward force reference, facilitating the execution of arbitrary movements by the wearer. In case of a sudden contact/load loss, a power-aware strategy is implemented to immediately eliminate the portion of external loading in the force reference. The adaptive compensation of the external loads is achieved through an electromyography interface. Instead, to react to sudden load releases, we set a power limit on the tendon, and continuously measure it through an encoder and a load cell connected with the cable. Two sets of experiments are designed to test the proposed load-releasing method on a bench-top setup with 2 kg, and 3.9 kg, and a human subject with 0.5 and 1 kg. Next, the overall scenario including load-compensation and load-releasing are carried out on eight human subjects with 0.5 and 1 kg loads to evaluate the release and compensation time, and the effort reduction with respect to non-powered exoskeleton case. Results show that the average compensation/release time (payload) among subjects is measured as 0.98/0.91 seconds (0.5 kg), and 1/0.86 seconds (1 kg). The average effort reduction among the subjects are also reported as 66.4%, and 67.11% for 0.5 kg, and 1 kg, respectively.**

***Index Terms*—Physically Assistive Devices, Wearable Robotics, Human Factors and Human-in-the-Loop.**

I. Introduction

DESPITE the significant progress achieved in robotics domain to automate and increase the flexibility of industrial tasks [1], [2], manual operations such as packaging [3] and assembly [4] still account for a large proportion of tasks in this area. To increase the productivity, ergonomics, and physical performance of the workers, in manual operations, wearable assistive devices have been developed for assisted walking [5], material handling [6], and sit-to-stand [7] applications in the last decade. They are mainly divided into two categories in terms of structure: rigid [8] and soft [9]. Moreover, rigid wearable devices can be categorized among each other as passive [10] and active [11].

Considering the active exoskeletons, they provide better control, wider flexibility and user comfort for load compensation in comparison to passive ones. In particular, when the device is controlled in force, feed-forward compensation can be employed for internal (e.g., users limb), and external (e.g., handheld tool) loads. In this way, user movements can be more comfortable since human intention-based triggering of arm movements (i.e., the force reference is updated depending on the position of the arm moved by the user) becomes simple and intuitive. For instance, in [12], the target is to assist the shoulder for overhead tasks in the industrial applications through an inflatable soft robot. The intention of the user is detected from the user's shoulder and trunk position. However, the main limitation of the system is to support the user above a certain shoulder threshold position due to a specific application. In another work [13], an elbow exosuit is controlled based on EMG (Electromyography) sensors, and the position of the elbow and a musculoskeletal model developed based on a nonlinear function to estimate the joint torque. Nevertheless, the method does not consider the load-releasing action, which is a crucial safety requirement for force-controlled systems.

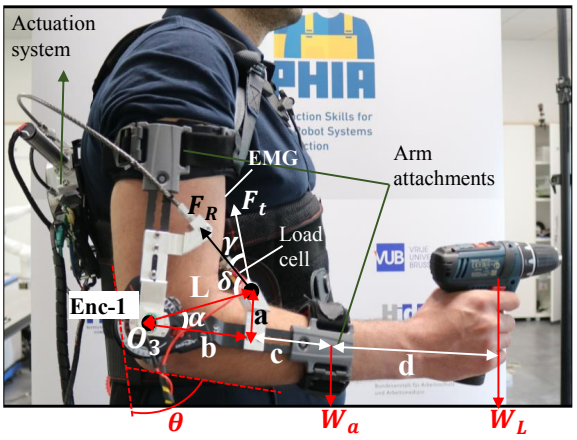

Fig. 1. The illustration of the developed effort-compensation device for elbow joint. The forearm width (a), the distance of fixed attachments from O_3 (b), the center of mass of the forearm (b+c), and the lever arm from hand (b+c+d) are determined as 50, 100, 150, and 300 mm for the subject-1 (S_1), respectively.

Alternatively, load compensation and release are conducted in [14] for elbow joint through sEMG attached on biceps and triceps. The increment in the former and the latter triggers the load compensation and release algorithm, respectively. To clarify, when the payload at hand is released, there is a sudden assistive force in an upward direction as the exoskeleton cannot recognize the load change at hand. The user then has to push the device using triceps to stop its movement. This initiates the load releasing phase. However, this strategy might disturb user's comfort and cause additional fatigue in the human limbs for long term operations. In another work, a shoulder support device is used to conduct load detection

Manuscript received: November, 14, 2022; Revised February, 17, 2023; Accepted May, 26, 2023. This paper was recommended for publication by Editor Angelika Peer upon evaluation of the Associate Editor Tamim Asfour and Reviewers comments. This work was supported by the European Unions Horizon 2020 research and innovation programme under Grant Agreement No. 871237 (SOPHIA).[1]Istituto Italiano di Tecnologia, Genoa, Italy. emir.mobedi@iit.it [2]Department of Electronics, Information and Bioengineering, Politecnico di Milano, Milano, Italy. [3]Dept. of Materials and Production, Aalborg University, Aalborg, Denmark. [4]Robotics Department, Hanyang University ERICA, Republic of Korea.

Digital Object Identifier (DOI): see top of this page.

IEEE Robotics and Automation Letters (RA-L) paper, presented at ICRA 2024, Yokohama, Japan. Cite as RA-L paper.

IEEE Robotics and Automation Letters (RA-L) paper, presented at ICRA 2024, Yokohama, Japan. Cite as RA-L paper.

through Myo Armband [6]. However, the developed controller is tested at 3 static conditions, and the release of the load from hand is performed by updating manually the assistive torque reference, which could be a limitation in dynamic tasks in industries. Additionally, payload estimation to control upper-body exoskeleton is conducted making use of force sensitive resistor (FSR) band in [15]. Due to the muscle contraction to compensate the payload, the band measures the normal forces and estimates the load through a machine learning algorithm. Even if the performed estimations are close to the actual loads, the method is tested at a static condition, and load releasing is not carried out.

Although several control strategies are developed for wearable devices to generate assistive torque based on EMG sensors, the load release phase has not been studied in the literature according to our knowledge. To clarify, the research question we address in this paper is when an object is released from the hand, how the assistive force reference of the exoskeleton can be adapted intuitively to the new payload (i.e. only arm compensation) without disturbing users' comfort?

In this paper, we propose a new control strategy to answer this question, and evaluate it on a recently developed elbow effort-compensation device [11], [16] for repetitive activities of daily living such as pick and place or painting task in industry. The actuation system of the device is attached distally from the user, and the generated assistive force is transferred to the wearer through the Bowden cable (see Fig. 1). In the actuation system design, a bungee elastic element is coupled with a ball-screw mechanism to change its elongation through a DC motor, and to transfer the assistive force to the arm in a compliant way. The device is controlled in force to enable movement transparency and to enhance user comfort when carrying external loads. The force reference is formed by the forearm weight and the load at hand, with the latter being detected and compensated online through an EMG based adaptive method. To do so, an assistive force is generated when the EMG of the biceps muscle goes above a threshold determined according to the user's muscle contraction under forearm compensation support. Subsequently, as soon as the EMG settles below this threshold, the load at hand is estimated based on the position of the elbow, the tendon force, and the geometry of the arm attachments.

Since the exoskeleton is controlled in force, sudden load release or similar disturbances may result in rapid device movements due to the feed-forward compensation forces, undermining users' safety. Hence, we propose and implement a power-aware control algorithm to decouple the load-related assistive forces from the controller. To achieve this, the power of the exoskeleton is calculated during the operation according to the weight of the user's forearm, the target payloads at hand, and the cable velocity. Next, a power threshold is assigned based on the user's cyclic motions. When the load is released from the hand, the power of the device increases suddenly above the threshold, and the external proportion of the reference load is eliminated. Hence, the exoskeleton will switch back to compensating the forearm weight and the user can comfortably move the own arm without interrupts.

In summary, we summarise the main contributions of this work below:

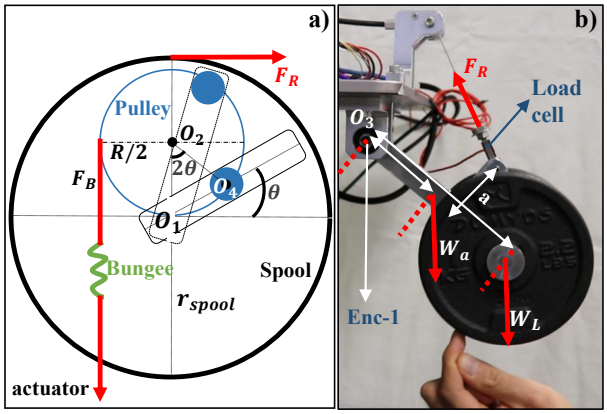

Fig. 2. The illustration of the a) working principle of the actuation system, and b) benchtop setup. r_{spool} is 88 mm, while R is 40 mm.

- Development and experimental verification of the power-aware control strategy to perform fast and smooth force adaptation to object releasing phase on a benchtop test with different payloads, different speeds, and different releasing positions ,
- Development of the load compensation algorithm using biceps EMG sensor output, and experimental validation of the load compensation and release algorithms on eight subjects for two different payloads at different elbow angles, and performance evaluation in terms of compensation/release time, and effort reduction with respect to non-powered exoskeleton case.

The rest of the paper is structured as follows. In section II, the design of the effort-compensation device and the working principle are briefly explained. In section III and IV, the controller design, and the experiments and results are presented. Finally, in section V, the conclusions are mentioned.

II. Effort-Compensation Device

The actuation system's working principle is presented in Fig. 2. An endless shape bungee ($\varnothing$10 mm) elastic element is connected to a plate in Fig. 3B, which is linearly moved by the ball-screw ($\varnothing$8 mm) and a DC motor (ECXTQ22XL, GPX22UP). The incorporation of the bungee brings about several advantages such as intrinsic damping and protecting the system from unexpected shocks. Thus, when assistance is needed, the bungee is elongated to generate an input torque around O_2 through the elastic force (F_B). Next, this input torque is transmitted to the spool through a roller that is coupled to the pulley. The force transmission is achieved with the help of a slot opened in the spool (see Fig. 2a). Hence, the DC motor adjusts the bungee elongation depending on the desired torque at the elbow. Finally, the output force (F_R) is transferred to the rigid link in Fig. 2b or the human arm in Fig. 1 with the help of the Bowden cable. It is also important to note that there is a 1:1 motion relation between the spool and the elbow position. A more detailed explanation of the actuation systems can be found in [11].

In the calculation of the elbow joint torque, the joint axis is assumed as a single-axis hinge joint, and symmetric with respect to both upper and lower arm limbs according to the

IEEE Robotics and Automation Letters (RA-L) paper, presented at ICRA 2024, Yokohama, Japan. Cite as RA-L paper.

IEEE Robotics and Automation Letters (RA-L) paper, presented at ICRA 2024, Yokohama, Japan. Cite as RA-L paper.

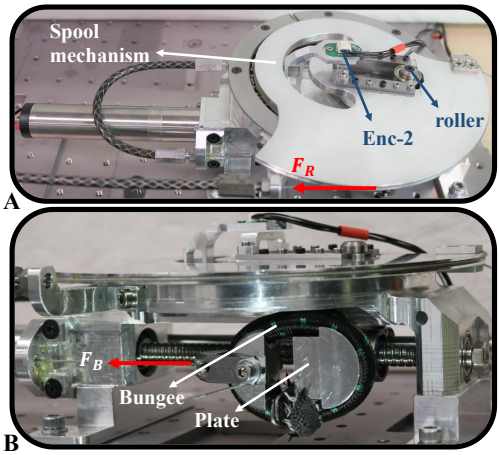

Fig. 3. The manufactured actuation system of the elbow effort-compensation device. Top view (A), and (B) Side view.

human model in [17], [18].

To calculate the desired torque at O_3 in Fig. 1, the following equality is written out:

$$\tau = \overbrace{W_L \sin(\theta) l_L}^{\tau_L} + \overbrace{W_a \sin(\theta) l_A}^{\tau_A}, \tag{1}$$

where W_L is the load carried by a human, and W_a is the forearm weight. Moreover, l_A, and l_L are the lever length for the arm $(b+c)$ and the load $(b+c+d)$, respectively. Hence, the force reference to support the above torque can be computed as follows:

$$F_R = \frac{\tau}{L\cos(\gamma)}, \quad \gamma = 90 - \alpha - (\theta/2), \tag{2}$$

$$\alpha = \arctan(a/b), \quad L = \sqrt{a^2 + b^2}, \quad \delta + \gamma = 90. \tag{3}$$

This force reference can be mathematically expressed as the following summation $F_R = F_A + F_L$, where F_A and F_L represent the force associated with the compensation of the weight of the forearm and an external load, respectively. Moreover, F_A, and F_L can be calculated by substituting only $\tau = \tau_A$, and $\tau = \tau_L$ in (2), respectively. Therefore;

$$F_L = \frac{W_L \sin(\theta) l_L}{L\cos(\gamma)}, \qquad F_A = \frac{W_a \sin(\theta) l_A}{L\cos(\gamma)}. \tag{4}$$

F_t in Fig. 1 is the vertical component of the F_R, and represented as $F_t = F_R \cos(\gamma)$.

III. Controller Design

The device is operated under force control. The controller is divided into two stages as the high-level controller (HLC), and the low-level controller (LLC). The load compensation and load release actions are included in the HLC. Then, the force references to achieve those tasks are generated and fed to the PID regulator. The output is acquired as the plate reference position (X_R). Accordingly, a conversion between X_R and reference position of the motor (φ_R), which is represented with C in Fig. 4, are carried out considering the gear ratio ($G = 3.9$) of the motor, and the ball-screw lead ($h = 3$ mm) in (5). Finally, φ_R is tracked by the PD regulator measuring the motor position (φ_M). This stage is identified as LLC.

$$X_R = h\frac{\varphi_R}{G}. \tag{5}$$

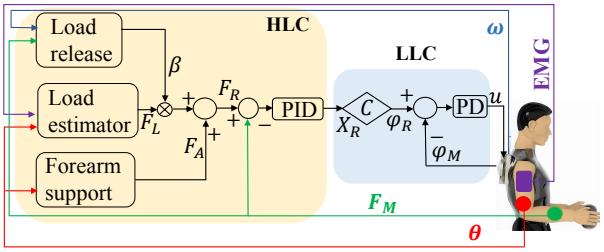

Fig. 4. The developed controller diagram for load compensation and release tasks. HLC and LLC represents high-level and low-level controller.

A. Load Compensation

The main purpose of the load compensation algorithm is to estimate the load at hand when the user holds it. First, an EMG is attached to the biceps, and only the forearm is supported (F_A) by the device. No load is held during this process at hand, and the user is asked to conduct cyclic movements. Next, the peak values of the measured EMG data are detected, and the root mean square of those peaks are computed. The resultant value is assigned as the minimum effort level (T_E) for each subject.

After T_E is identified, any external load introduced to the system (user holds an object in the hand), will result in an increase in the EMG signal. Thereby, the load estimation is initiated generating F_L as a ramp function on the tendon to assist the user. For the derivation of the slope of this ramp function, first, maximum value of F_L in (4) is computed considering the load estimation parameters. To begin with, θ_C (applicable elbow angle) is identified as minimum $50°$ ($\theta_{C_{MIN}}$) or above for the load estimation since the EMG values change depending on the arm configuration. As expected, it is very low when the arm is at fully extended position, which means $\theta = 0$ in (1), and the effort (τ) in elbow joint is close to zero (This prevents conducting load estimation).

After the parameter determination, $F_{L_{MAX}}$ is computed as ≈ 30 N through (4) by substituting $W_L = W_{Max} = 10$ N, $\theta = \theta_{C_{MIN}}$, and other parameters (i.e. l_L, L, and γ using a, b, c, d in Table.I). We targeted to generate $F_{L_{MAX}}$ in 1 second for proof-of-concept. As the controller update rate is 1 kHz, F_{inc} (slope of the ramp function) can be computed as follows:

$$F_L = F_{L_P} + \overbrace{F_{L_{MAX}}}^{F_{inc}} \frac{t_i}{t_t}, \qquad W_L = \frac{F_L L\cos(\gamma)}{\sin(\theta) l_L} \tag{6}$$

where t_i, t_t, and F_{L_P} represents the controller update rate, targeted load estimation time, and the previous value of F_L, respectively. F_{inc} can be calculated as 0.03 N in (6). Next, W_L is isolated from (4), and written in (6). F_L is increased (starting from 0) adding F_{inc} on the F_{L_P} to compute the estimated load in this equation.

During this interval, when the EMG reduces below T_E, the force increment (i.e. F_{inc}) is terminated, and the load is estimated. Therefore, F_L is updated according to the estimated load throughout the elbow motion range in (4), and the EMG signal is eliminated from the controller. Noteworthy, in recent works, the EMG is used for assistance in which its value is multiplied with a gain that has to be regulated during the operation by the wearer [19], or a fixed gain [6] potentially increasing the mental load of the wearer. Instead, our approach

IEEE Robotics and Automation Letters (RA-L) paper, presented at ICRA 2024, Yokohama, Japan. Cite as RA-L paper.

does not require EMG signal during the task as the load is estimated only once through the arm attachment geometry, and the position of the elbow. Additionally, since the main design idea of the device is to reduce the effort for repetitive tasks, the success rate for load estimation is assumed as a minimum 70% of the actual load. As the upper limit of the load estimation, +1.5 N is added to the actual load to avoid excessive support on the arm (e.g., if the actual load is 10 N at hand, the estimation of W_L is acceptable up to 11.5 N).

B. Power-Aware Load Releasing

As previously mentioned, one of the challenges of assisting people using wearable devices with force control is to adapt the exoskeletons' response when the object, held by the user, is released from the hand. At that instant, the device pushes the arm in an upward direction since the force reference is generated for the load and the forearm.

To achieve a fast force reference transition to only forearm support, yet smooth and intuitive, we correlate the output power and the force reference of the exoskeleton. Starting from the former one, it is supplied through a tendon cable (wrapped around the spool) to the user. Therefore, the calculation of the power (P_{Exo}) is conducted based on the velocity ($\dot{x}$) and the force (F_M) of the tendon in (7).

$$P_{Exo} = F_M \dot{x}, \qquad \dot{x} = r_{spool}\omega \tag{7}$$

To compute the $\dot{x}$, the spool velocity (ω) and radius are taken into account, and their units are considered in radian, and mm, respectively.

In the method, first, a power threshold (P_{Max}) is set taking into account the max payload (W_{Max}) and the elbow velocity that the exoskeleton shall generate to assist the user for a task. Next, when contact is lost between the object and the user, the P_{Exo} goes beyond the P_{Max} due to a sudden load change. Accordingly, the force reference for the load (F_L) is multiplied by the coefficient β (see Fig. 4), which becomes zero to eliminate the portion of F_L in (8). Hence, only arm support (F_A) is fed to the system as the force reference to achieve an adaptation to the load change. Therefore;

$$F_R = F_L\beta + F_A \tag{8}$$

$$\beta = \begin{cases} 0, & \text{if } P_{Exo} > P_{Max} \\ 1, & \text{otherwise.} \end{cases} \tag{9}$$

Consequently, the proposed method allows the wearer to perform motions with W_{Max} unless the P_{Max} is exceeded. Moreover, the reason for the unidirectional power threshold is that the unsafe movement (pushing in an upward direction) can only take place in flexion movement since the effort-compensation device stores the energy in this direction by tensioning the bungee. For assistance in extension, this stored elastic energy is used by releasing the bungee depending on the arm position. Since the sign of the power in flexion movement is positive due to the direction of F_M and $\dot{x}$, the P_{Max} is assigned as a positive value expressed in the next section.

IV. Experiments & Results

The performance of the presented control approach is validated through two experimental studies. The first experimental study focuses solely on the validation of the power-aware load release on a bench-top setup (see Fig. 2b), whereas the second one validates the load estimation method and the power-aware load release on 8 healthy right-handed human subjects (28 ± 3 years old), which was carried out at the Human-Robot Interfaces and Physical Interaction (HRII) Lab, Istituto Italiano di Tecnologia (IIT), and approved by the ethics committee Azienda Sanitaria Locale (ASL) Genovese N.3 (Protocol IIT HRII SOPHIA 554/2020).

In both experiments, the same actuation system is used. However, in the benchtop test, the device is fixed on a table (see Fig. 3A), and connected through a tendon to a rigid link designed to mimic the human arm dimensions (see Fig. 2b). Also, different payloads (max 3.9 kg) are hung on it to reach a similar max F_R value as the human arm with targeted loads (0.5 and 1 kg). On the other hand, in the human tests, the effort-compensation device is worn by the participants (see Fig. 1 for S_1), and the data including T_E, P_{Max}, and W_a are illustrated in Table.I. A simple calibration phase is designed to measure them.

In both tests, force references are generated using (4). For the benchtop test, l_A, l_L, and W_a are considered as 127 mm (lever length between O_3 and the point of W_a), $b + c$ (load lever length), and 0.42 kg, respectively. Moreover, for the human experiments, l_A, and l_L are taken into account as it is stated in II. Additionally, a load cell (FUTEK-LSB201) is used in both experiments to measure the tendon force, and 2 Hz Butterworth low-pass filter is used to filter the data. Two encoders are attached to measure the angular position (θ for link and elbow), and the velocity of the spool (ω). A motor driver and a data acquisition card, which are communicating through EtherCAT at 1 kHz, are integrated to control the device in MATLAB®/Simulink Real-Time interface. A PID controller is employed for force control ($K_{P_f} = 0.1, K_{I_f} = 6, K_{D_f} = 0.002$), and the output of this controller is X_R, which is tracked by the motor through a PD regulator ($K_P = 12000, K_D = 5$).

Throughout the human experiments, the muscular activities of biceps brachii, which is the main muscle for flexion movement, are acquired utilizing the wireless EMG system of Delsys Trigno platform by Delsys Inc (Natick, MA, United States). The EMG is acquired at 100 Hz, and post-processed with a second order high-pass filter with 0.1 Hz. Then, full-

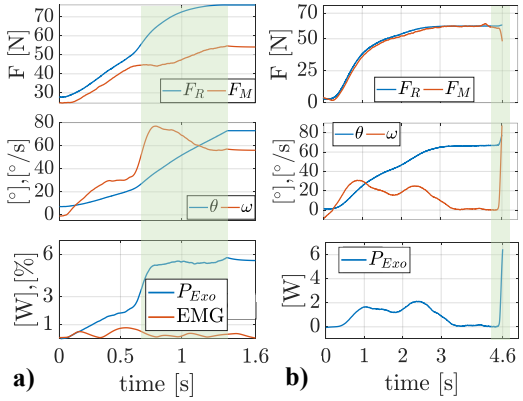

Fig. 5. a) The experiment-1 results, where no power limit is defined in the exoskeleton, and 10 N load is released by S_1 to monitor force jump on the tendon. b) The experiment-A results where the link is hung 2 kg payload without setting P_{Max} in the benchtop setup.

IEEE Robotics and Automation Letters (RA-L) paper, presented at ICRA 2024, Yokohama, Japan. Cite as RA-L paper.

IEEE Robotics and Automation Letters (RA-L) paper, presented at ICRA 2024, Yokohama, Japan. Cite as RA-L paper.

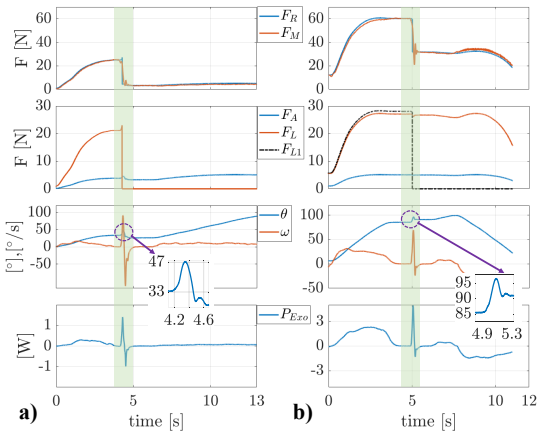

Fig. 6. a) The experiment-B results where the load releasing is tested under 2 kg payload on benchtop setup with $P_{Max} = 1$ W, and b) The experiment-C results in which the load releasing is performed under 3.9 kg payload on the benchtop with $P_{Max} = 3$ W. Green area shows the time interval of load-releasing. The dashed purple circle illustrates the load-releasing phase for zoomed-view.

wave rectification is implemented, and finally, a second-order low pass filter is applied with 2.5 Hz.

A. Benchtop Experimental Protocol

Three experiments are conducted to validate the developed power-aware load releasing method. Experiment-A is designed without defining a power limit. First, the user varies arbitrarily the link position under 2 kg payload to represent the flexion/extension movement. Then, this load is removed suddenly from the link at a position to show the problem of sudden power increment on the cable. In experiment-B, the power threshold is defined as 1 Watt (W) based on a cyclic motion for 2 kg load with the desired velocity of the link, which is $10°/s$ (ω_{d1}). The user is asked to conduct flexion/extension movement on the link with this velocity by following the avatar that is created in MATLAB®. Finally, the load is taken out at around 35°. In experiment-C, the payload is increased to 3.9 kg, and the link position is changed with $25°/s$ (ω_{d2}) by the user using the same simulation (different velocity) mentioned above. Also, the power threshold is set as 3 W, and the user is asked to remove 2 kg load at around 90° to show the performance of the controller at a different load-releasing position.

B. Benchtop Experimental Results

In Fig. 5b, the results of experiment-A are presented. At $t = 4.5$ s, the load is removed, and ω reaches up to 80°/s showing an unsafe movement due to the generated force reference for the load. When it comes to experiment-B results in Fig. 6a, at $t = 4.2$ s, the load is taken out, and, β becomes zero since P_{Exo} exceeds the power limit (illustrated in green area) according to the condition in (8). Hence, the portion of F_L is eliminated, and the device is fed only the link mass compensation (F_A).

In experiment-C results (see Fig. 6b), since the load on the link is increased to 3.9 kg, the F_R reaches up to 60 N. Here, F_L is considered for 2 kg and 1.9 kg, separately, and only the former one is multiplied by β. Therefore, it can be clearly seen in Fig. 6b (second row) that the dashed line and the orange line move together until $t = 5$s (pointed out in green area) in which the load-releasing starts. Then, when the power goes beyond the assigned limit, the force reference that belongs to 2 kg (F_{L1}) is multiplied by β, and its effect on F_R is terminated. Then, the user conducts free motion with the remaining load. Important to note that, the adaptation time to new force reference in experiment-B and experiment-C are monitored as ≈ 0.4s, even though the load is released at 33° and 85° (see the zoomed views in Fig. 6). During this interval, the link position increases 13°, and then settles to its previous position with minimal error, which is quite a rapid adaptation since both velocity and force of the tendon are taken into consideration to limit the power. Additionally, the root mean square (RMS) error of the tendon force ($F_R - F_M$) for experiment-B, and experiment-C are computed to be 0.84 N, and 1.91 N, respectively.

C. Human Experimental Protocol

The procedure is initiated with a calibration phase. First, the subjects' forearm weight is measured to estimate F_A, and to separate the effect of external load on the biceps muscle when the user holds a load. In other words, if a constant W_a is assigned for all subjects, and if this value is lower than the actual one, the users' effort may increase. Eventually, this could be sensed by EMG as a load at hand. Also, if the aforementioned weight is higher than another user's forearm weight, the device could apply excessive support to the user. Due to these reasons, the subjects are asked to let their arm be compensated by the exoskeleton at 90°. Making use of the measured tendon force and elbow position, W_a values are computed through (4) for each participant.

After this step, the device is fed only F_A (see Fig. 4) using the computed W_a, and the subjects follow the avatar (the similar simulation mentioned in IV-A) that performs the movement with ω_{d1}. Throughout this period, the normalized EMG values, which are acquired through maximum voluntary contraction (MVC [%]), are measured to compute the T_E (The details of the computation is mentioned in III-A). Later on, participants are given W_{Max} as the load, and F_L is fed

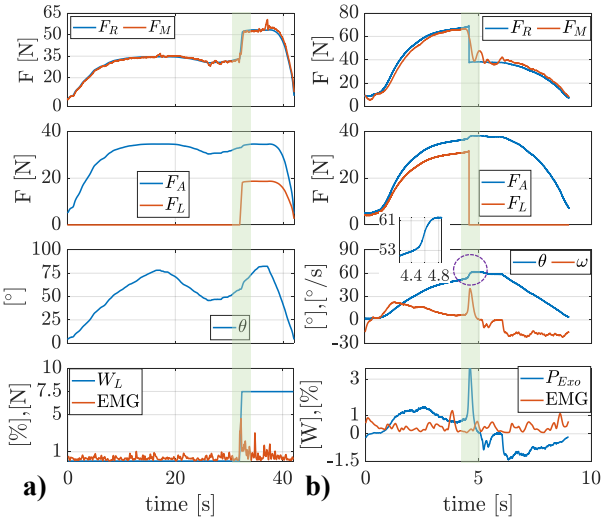

Fig. 7. (a) The experiment-2 results of S_1 where only load-compensation algorithm is tested for 1 kg load, and then only load-release is performed for the same payload on S_1 with $P_{Max} = 3$ W in experiment-3 (b).

IEEE Robotics and Automation Letters (RA-L) paper, presented at ICRA 2024, Yokohama, Japan. Cite as RA-L paper.

IEEE Robotics and Automation Letters (RA-L) paper, presented at ICRA 2024, Yokohama, Japan. Cite as RA-L paper.

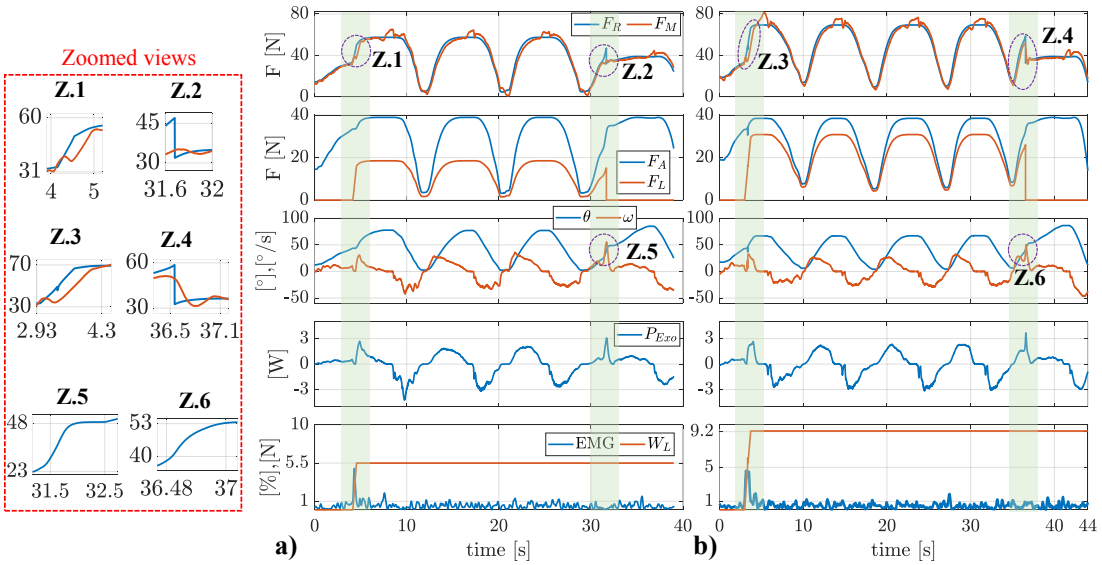

Fig. 8. The results of experiment-4 where both load compensation and load release algorithms are tested for S_1 with 0.5 kg (a), and 1 kg (b). The green area shows the time interval of load-compensation and load-releasing. P_{Max} is defined for two payloads to be 3 W. Dashed purple circle points out the load transition phases.

to device for this payload through (4). During this period, subjects pursue an avatar, which conducts flexion/extension movements with ω_{d2}, while measuring the power of the exoskeleton to record the P_{Max} value. At the end of this process, T_E, P_{Max}, and W_a parameters are determined for each subject. The reason why P_{Max} values (see Table.I) differ for the subjects although there is a small difference in their forearm weight is because of the different elbow velocities. This happens due to the visual feedback (avatar) that subjects try to follow, and possible velocity errors have an effect on the power values. 0.5 W is also added to the measured power values as tolerance in case of sudden reflexive movements that might occur during the experiments.

To start with, experiment-1 is conducted to monitor the sudden force jump on the cable when W_{Max} is released from subject-1's hand. No power limit is defined, and the user is assisted with this load and forearm weight. During the test, the EMG data of the subject is also recorded to make sure that there are no anticipatory movements. In experiment-2, only the load compensation algorithm is verified on S_1 for the same payload. The subject is asked to perform flexion movement following the avatar that conducts the desired motion with ω_{d1}. When the arm reaches the range of θ_C, the load is released to the subject-1's hand smoothly, and it is balanced instantaneously by S_1, which initiates the load compensation algorithm. Afterward, experiment-3 is carried out to validate only the load-releasing algorithm on the same subject for the same payload. To do that, the participant is informed to perform deliberate movement following an avatar that carries out the desired motion with ω_{d2}. Then, the load is released at a position without contracting the arm (i.e. naturally).

Next, experiment-4 is conducted to verify the developed load-compensation and load-releasing algorithms together in the same season through two different payloads (0.5 kg and 1 kg) on 8 subjects. The participants perform the same protocol mentioned in experiment-2 (load-compensation), and experiment-3 (load-releasing), consecutively. Finally, experiment-5 is carried out, and the subjects execute flexion/extension movements with ω_{d2} following the avatar. In this case, the exoskeleton is powered off, and the cable is slacked. The goal is to observe the effort reduction on the biceps muscle thanks to the load-compensation and release algorithm. Throughout the human experiments, 10 minutes rest is given to the subjects in between 0.5 kg and 1 kg payload tests to minimize the development of fatigue.

D. Human Experimental Results

According to the experiment-1 result in Fig. 5a, the subject starts doing flexion movement until $t = 0.8$ s, and then releases the object. It is clear that the device moves the arm $\approx 60°$ in 1 second (no anticipatory movements are observed on EMG data), and then the system is powered off immediately. As expected, P_{Exo} also sharply rises up to 6 W, and this behavior is not safe. Thus, P_{Max} is defined in experiment-3 (see Fig. 7b), and the results show that when the load is released, the device adapts to only F_A eliminating the F_L in 0.4 s thanks to the β term in the power-aware control strategy.

When the experiment-2 results are investigated in Fig. 7a, the user performs deliberate movement until $t = 30$s. After that, the object is held by the user, and EMG goes above T_E. This triggers the load-compensation algorithm, and F_L starts to increase until EMG reduces below the minimum effort level. After that, W_L is computed, and F_L is included in the force reference together with F_A (Fig. 7a). The summation of these two terms is presented in the first row of the same figure (F_R).

Regarding the experiment-4 results in Fig. 8, S_1 executes flexion movement until $t = 4$ s (a), and $t = 2$ s (b). During those periods, P_{Exo} does not exceed the P_{Max}, and F_L is zero since EMG is below T_E. Hence, only F_A is transferred to the wearer. When the load is released to the users' hand, the EMG increases (most bottom plots), and this initiates the load-estimation algorithm by generating F_L. As soon as EMG settles below T_E, the W_L is computed. Then, S_1 performs free-motions, and releases the load around $t = 30$ s, and

IEEE Robotics and Automation Letters (RA-L) paper, presented at ICRA 2024, Yokohama, Japan. Cite as RA-L paper.

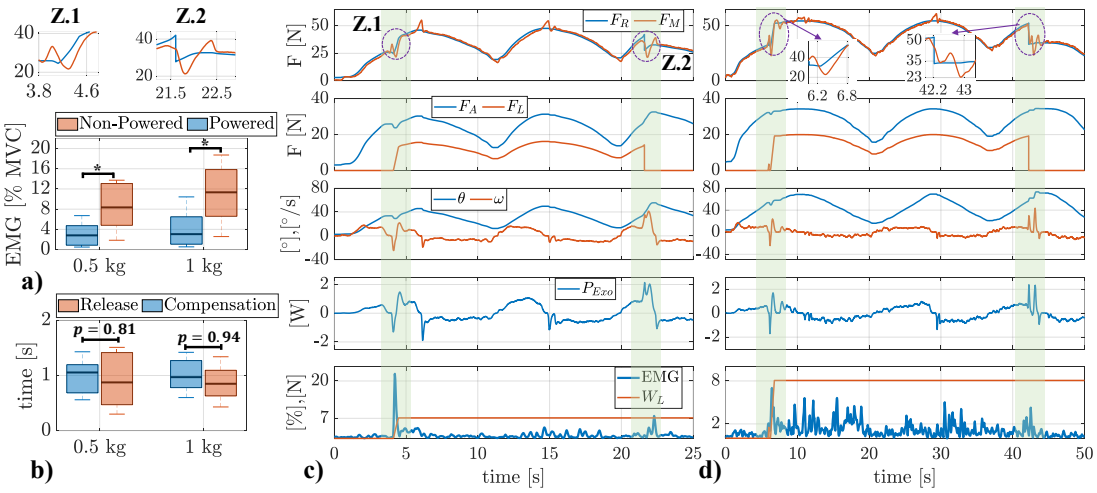

Fig. 9. The results of experiment-4 in which both load compensation and load release are performed for S_2 (c), and S_3 (d) with 1 kg. The comparison of effort-reduction for with and without exoskeleton among 8 subjects for 0.5 and 1 kg (a), and the load-compensation and releasing time (b). The green area shows the load transition phases. $^*p < 0.05$.

$t = 35$ s for 0.5 kg, and 1 kg, respectively. At those instants, P_{Exo} surpasses the P_{Max}, and F_L becomes zero. Important to note that, although the objects are released at different positions (see Z.5 and Z.6) the adaptation time to only arm support during the load-releasing is around 0.6s.

The results of S_2, and S_3 for the same experiment are shown in Fig. 9. In this case, the P_{Max}, and T_E are different from S_1 (see Table.I), which changes the EMG trends among subjects for the load-compensation phases. The fluctuations on F_M during the load-releasing phase comprises from the bungee elastic element integrated in the actuator design. To clarify, since F_L is eliminated from F_R as a step signal, the bungee acts as a mechanical filter between motor and the arm, transmitting this sudden change of motor to the user in a compliant way (shock absorbing). Additionally, the load-releasing and load-compensation time values are reported through zoomed views in Fig. 8, and Fig. 9. The load change duration is taken into account when F_M settles on F_R after the load-releasing or compensation phase. Throughout the load-releasing phases, the effort on EMG is monitored below T_E value, which demonstrates that the device naturally adapts the assistance to the remaining payload without disturbing the users' comfort.

Finally, the data of all subjects for experiment-4 are presented in Table.I, and statistical analysis is carried out in MATLAB®for the effort reductions, load compensation time (t_1), and load release time (t_2) with the level of significance 0.05. If p (p-value) is above this value, this means that the data is not significantly different. Otherwise, there is a significant difference among the selected data. For the effort reduction results, Wilcoxon rank sum test is carried out since the data is not normally distributed. p is acquired to be less than 0.05 for both payloads. This concludes that the data in between powered and non-powered cases are significantly different, which is an expected outcome. When it comes to t_1, and t_2, Wilcoxon signed rank test is conducted, and the desired median value of t_1, and t_2 is applied to be 1 second (targeted load-estimation time (t_t), in (6)). According to the results, p (time) values are acquired to be 0.81 (t_1), and 0.94 (t_2), for 0.5 kg and 1 kg, respectively. This demonstrates that the results are statistically not different, showing trivial differences around the desired median value. Furthermore, the mean value±standard deviation (payload) of the t_1 are calculated 0.98 ± 0.31 (0.5 kg), and 1 ± 0.29 (1 kg), and it is also computed for t_2 to be 0.91 ± 0.49 (0.5 kg), and 0.86 ± 0.3 (1 kg). The reason why the load-releasing time for 0.5 kg is slightly higher than 1 kg (see Fig. 9) is because P_{Max} is assigned by considering 1 kg payload at the beginning instead of the online estimated loads. Thus, the worst-case scenario is taken into account in the test procedure. Lastly, the mean value±standard deviation (payload) of the W_L estimations are computed as 5.59 ± 0.52 N (5 N), and 8.74 ± 1.08 N (10 N) both of which are under the tolerance of the desired W_L values. Additionally, the mean value±standard deviation (payload) of the minimum/maximum elbow positions [°] are reported to be $11.97 \pm 5.31/74.2 \pm 7.76$ (0.5 kg), and $10.63 \pm 7.27/69.3 \pm 10.55$ (1 kg). The reason for the variations on θ_{Max} is that the participants are informed to conduct deliberate movement while following the avatar. This allows us to acquire similar arm velocities as that of the avatar, and eventually to keep the P_{Exo} below P_{Max} value unless there is load release action.

V. Conclusions & Future Study

In this work, we presented a new control strategy for sudden unloading tasks through the power of the force-controlled elbow effort-compensation device. First, the developed method is tested on a benchtop setup hanging 2 kg and 3.9 kg payloads, at different link speeds, and different load-releasing positions. Then, load estimation is also accomplished through a control strategy utilizing EMG sensor data attached to the user's biceps muscle. Later on, load-releasing and load-compensation operations are carried out separately on a subject. Finally, the overall scenario is verified for both actions consecutively in the same experiment on 8 participants with different payloads, different arm speeds, and different load-releasing arm positions. In addition, the subjects performed the desired tasks through the simulation without the exoskeleton to show the strength of the developed control method in terms of effort reduction.

IEEE Robotics and Automation Letters (RA-L) paper, presented at ICRA 2024, Yokohama, Japan. Cite as RA-L paper.

TABLE I
EXPERIMENT-4 RESULTS AND THE DETERMINED THRESHOLDS OF THE SUBJECTS

$a, b, c, d: 50, 100, 50, 150$ [mm]	**Subject-1**		**Subject-2**		**Subject-3**		**Subject-4**		**Subject-5**		**Subject-6**		**Subject-7**		**Subject-8**	
T_E [%], P_{Max} [W], W_a [N]	1, 3, 27		2, 2, 24		2, 2, 25		3, 1.5, 24		9, 3.2, 25		3.5, 3, 22		4, 2.5, 25		7, 2.5, 21	
Payload [kg]	**0.5**	**1**	**0.5**	**1**	**0.5**	**1**	**0.5**	**1**	**0.5**	**1**	**0.5**	**1**	**0.5**	**1**	**0.5**	**1**
W_L [N]	5.5	9.2	4.6	7.1	5.1	8.07	6.2	7.58	6.05	8.5	5.9	9.8	5.8	10.1	5.5	9.5
t_1 [s]	1	1.36	0.56	0.68	0.61	0.6	1.16	1.42	0.76	0.92	1.43	0.88	1.23	1.02	1.11	1.18
t_2 [s]	0.4	0.64	1.37	1.13	0.72	0.78	1.46	1.34	0.3	0.62	1.51	0.92	0.54	0.43	1.03	1.06
θ_{Max} [°]	77.3	70.9	63.5	50.1	71.2	69.4	66.6	65	82.2	84.7	77.4	64.9	69.4	68.3	85.8	80.8
θ_{Min} [°]	1.6	1.8	15.4	9.5	13.2	16.4	9.9	9.3	7.2	9.1	16.8	2.8	16.2	11.4	15	24.5
Force Error [N]	3.26	4.06	2.15	2.25	2.62	1.86	1.55	1.64	3.39	3.35	2.65	3.06	4.84	3.72	3.51	4.65
Effort Reduction [%]	87.03	89.4	45	54.4	87.1	88.4	73.2	68.4	51.05	63.1	62.5	75.2	71.01	44.2	54.4	53.04

T_E, P_{Max}, W_a, W_L, t_1, t_2 represent the minimum effort level, the maximum power, measured forearm weight, estimated load, load compensation time, and load release time, respectively. a, b, c, d are the dimensions of the arm attachments in mm and identified the same value for all the subjects. θ_{Max}, and θ_{Min} are the measured maximum and minimum elbow positions of the subjects.

Results show that the mean value±standard deviation of the effort reduction [%] among subjects for 0.5 kg and 1 kg is 66.42 ± 15.92, and 67.11 ± 16.49, respectively. In addition, the average load compensation/release time for the two payloads is acquired as $0.99/0.89$ s. As expected, the load-releasing time on benchtop setup is sharply lower than human, measured as 0.4 s. The reason for this is due to the compliant coupling between the exoskeleton and humans as well as load estimation errors, which causes to demonstrate lower forces on the tendon, and eventually increases the time duration to reach the assigned power limit. However, we believe that the implementation of power in the area of exoskeletons for load-transition in force control has significant advantages since we intuitively change the force reference without increasing the effort on humans or setting manually the payload as it has done already in the literature [14], [6]. Additionally, the method can be applied in any force/torque controlled assistive device including rehabilitation and, active daily life exoskeletons for different limbs such as shoulder, back, or even knee, as long as the torque and the velocity of the joint are measured (minimum requirement) for the computation of P_{Exo}. As a future study, we aim to conduct the load compensation and release algorithm in different experimental conditions such as blindfolded to monitor the t_1, and t_2 values under unpredictable perturbations as in [20]. Also, we plan to test the algorithm in more repetitive use cases such as pick and place in a real industrial scenario.

REFERENCES

[1] E. Mobedi, N. Villa, W. Kim, and A. Ajoudani, "An adaptive control approach to robotic assembly with uncertainties in vision and dynamics," in *2020 29th IEEE International Conference on Robot and Human Interactive Communication (RO-MAN)*, 2020, pp. 144–150.

[2] N. Villa, E. Mobedi, and A. Ajoudani, "A contact-adaptive control framework for co-manipulation tasks with application to collaborative screwing," in *2022 31st IEEE International Conference on Robot and Human Interactive Communication (RO-MAN)*, 2022, pp. 1131–1137.

[3] M. Napolitano, "2012 warehouse/dc operations survey: mixed signals," *Logistics management (Highlands Ranch, Colo.: 2002)*, vol. 51, no. 11, 2012.

[4] B. Vanderborght, *Unlocking the potential of industrial humanrobot collaboration: A vision on industrial collaborative robots for economy and society*. Publications Office of the European Union, 2 2020.

[5] S. Lee, S. Crea, P. Malcolm, I. Galiana, A. Asbeck, and C. Walsh, "Controlling negative and positive power at the ankle with a soft exosuit," in *2016 IEEE International Conference on Robotics and Automation (ICRA)*, 2016, pp. 3509–3515.

[6] D. Park, C. Di Natali, D. G. Caldwell, and J. Ortiz, "Control strategy for shoulder-sidewinder with kinematics, load estimation, and friction compensation: Preliminary validation," *IEEE Robotics and Automation Letters*, vol. 7, no. 2, pp. 1278–1283, 2021.

[7] Y. Zhang, A. Ajoudani, and N. G. Tsagarakis, "Exo-muscle: A semi-rigid assistive device for the knee," *IEEE Robotics and Automation Letters*, vol. 6, no. 4, pp. 8514–8521, 2021.

[8] B. K. Dinh, M. Xiloyannis, C. W. Antuvan, L. Cappello, and L. Masia, "Hierarchical cascade controller for assistance modulation in a soft wearable arm exoskeleton," *IEEE robotics and automation letters*, vol. 2, no. 3, pp. 1786–1793, 2017.

[9] J. L. Samper-Escudero, A. Gimnez-Fernandez, M. . Snchez-Urn, and M. Ferre, "A cable-driven exosuit for upper limb flexion based on fibres compliance," *IEEE Access*, vol. 8, pp. 153 297–153 310, 2020.

[10] M. Asgari, P. T. Hall, B. S. Moore, and D. L. Crouch, "Wearable shoulder exoskeleton with spring-cam mechanism for customizable, nonlinear gravity compensation," in *2020 42nd Annual International Conference of the IEEE Engineering in Medicine & Biology Society (EMBC)*. IEEE, 2020, pp. 4926–4929.

[11] E. Mobedi, W. Kim, E. De Momi, N. G. Tsagarakis, and A. Ajoudani, "A soft assistive device for elbow effort-compensation," in *2021 IEEE/RSJ International Conference on Intelligent Robots and Systems (IROS)*. IEEE, 2021, pp. 9540–9547.

[12] Y. M. Zhou, C. Hohimer, T. Proietti, C. T. ONeill, and C. J. Walsh, "Kinematics-based control of an inflatable soft wearable robot for assisting the shoulder of industrial workers," *IEEE Robotics and Automation Letters*, vol. 6, no. 2, pp. 2155–2162, 2021.

[13] N. Lotti, M. Xiloyannis, G. Durandau, E. Galofaro, V. Sanguineti, L. Masia, and M. Sartori, "Adaptive model-based myoelectric control for a soft wearable arm exosuit: A new generation of wearable robot control," *IEEE Robotics & Automation Magazine*, vol. 27, no. 1, pp. 43–53, 2020.

[14] M. Hosseini, R. Meattini, A. San-Millan, G. Palli, C. Melchiorri, and J. Paik, "A semg-driven soft exosuit based on twisted string actuators for elbow assistive applications," *IEEE Robotics and Automation Letters*, vol. 5, no. 3, pp. 4094–4101, 2020.

[15] M. R. U. Islam and S. Bai, "Payload estimation using forcemyography sensors for control of upper-body exoskeleton in load carrying assistance," *Modeling, Identification and Control*, vol. 40, no. 4, pp. 189–198, 2019.

[16] E. Mobedi and A. Ajoudani, "Dispositivo di assistenza al movimento per larticolazione del gomito, (Patent ID: 102021000023081) ," *Available online: http://hdl.handle.net/11311/1213969, (accessed on October 2022)*.

[17] L. Kapandji, "The physiology of the joints-annoted diagrams of the mechanics of the human joints," *Upper limb*, pp. 108–129, 1982.

[18] J. C. Perry, J. Rosen, and S. Burns, "Upper-limb powered exoskeleton design," *IEEE/ASME transactions on mechatronics*, vol. 12, no. 4, pp. 408–417, 2007.

[19] T. Lenzi, S. M. M. De Rossi, N. Vitiello, and M. C. Carrozza, "Intention-based emg control for powered exoskeletons," *IEEE Transactions on Biomedical Engineering*, vol. 59, no. 8, pp. 2180–2190, 2012.

[20] A. Forghani, R. Preuss, and T. Milner, "Postural response characterization of standing humans to multi-directional, predictable and unpredictable perturbations to the arm," *Journal of Electromyography and Kinesiology*, vol. 32, pp. 83–92, 2017.

IEEE Robotics and Automation Letters (RA-L) paper, presented at ICRA 2024, Yokohama, Japan. Cite as RA-L paper.